Active particle in one dimension subjected to resetting with memory

Denis Boyer[1] and Satya N. Majumdar[2]
[1]*Instituto de Física, Universidad Nacional Autónoma de México, Ciudad de México 04510, México*
[2]*LPTMS, CNRS, Université Paris-Sud, Université Paris-Saclay, 91405 Orsay, France*

(Received 20 December 2023; accepted 26 March 2024; published 6 May 2024)

The study of diffusion with preferential returns to places visited in the past has attracted increased attention in recent years. In these highly non-Markov processes, a standard diffusive particle intermittently resets at a given rate to previously visited positions. At each reset, a position to be revisited is randomly chosen with a probability proportional to the accumulated amount of time spent by the particle at that position. These preferential revisits typically generate a very slow diffusion, logarithmic in time, but still with a Gaussian position distribution at late times. Here we consider an active version of this model, where between resets the particle is self-propelled with constant speed and switches direction in one dimension according to a telegraphic noise. Hence there are two sources of non-Markovianity in the problem. We exactly derive the position distribution in Fourier space, as well as the variance of the position at all times. The crossover from the short-time ballistic regime, dominated by activity, to the long-time anomalous logarithmic growth induced by memory is studied. We also analytically derive a large deviation principle for the position, which exhibits a logarithmic time scaling instead of the usual algebraic form. Interestingly, at large distances, the large deviations become independent of time and match the nonequilibrium steady state of a particle under resetting to its starting position only.

DOI: 10.1103/PhysRevE.109.054105

I. INTRODUCTION

Consider a single particle diffusing on a line with diffusion constant D. In Ref. [1] this diffusive dynamics was studied in the presence of an additional resetting move that is history dependent. In this model, in addition to diffusion, the particle also undergoes resetting with rate r to a previously visited position according to the following stochastic rule. At any given time t, the particle chooses at random, i.e., with probability density $1/t$, a preceding time $t' \in [0, t)$ and resets to the position at which it was located at t'. Thus the resetting move tends to dynamically localize the particle near the positions that are most often visited, as the probability to choose a particular site for revisit is proportional to the accumulated occupation time at that site. The position distribution of the particle was found to approach a Gaussian form at late times t, with the variance growing in a slow anomalous way as $(2D/r)\ln(rt)$ asymptotically [1]. This very slow dynamics emerges from resetting induced memory effects: The particle becomes sluggish and "reluctant" to move away from its familiar territory that it has already visited. Moreover, the position distribution is always time dependent and does not approach a stationary state at late times, in contrast to diffusion with stochastic resetting to a single site [2,3]. This simple model was able to fit quantitatively several statistical properties of the movements of capuchin monkeys in the wild [1], providing further evidence that many animal species use sophisticated cognitive skills to explore their environment and that memory should be incorporated in biological random-walk models [4–10].

Various other generalizations of this simple exactly solvable model have been studied in recent years [11–15]. Moreover, central and local limit theorems have been rigorously established for an extended class of memory walks of this type (including cases with fading memory), the proofs being based on a mapping onto weighted random recursive trees [16]. The large deviations of these walks were the focus of Ref. [17]. A quenched large-deviation principle was proven when the sequence of resetting times was given and acting as a disordered environment [17].

In this paper we consider an active version of this model where the resetting dynamics is similar to the above, except that between resets the particle undergoes a self-propelled active dynamics in one spatial dimension with velocities $\pm v_0$, instead of ordinary diffusion. Correlated random walks have been widely used to model the directional persistence which characterizes the movements of many animals and cells (see, e.g., [18] for a review). The state of the particle at time t is now specified by two degrees of freedom: the position and the velocity. More precisely, in a small time dt, with probability $1 - r dt$, the position $x(t)$ of the particle gets incremented by $v_0\sigma(t)dt$, where $\sigma(t) = \pm 1$ is a telegraphic noise that switches between $+1$ and -1 with a constant rate γ. The driving noise has a two-time correlation function that decays exponentially with the time difference,

$$\langle v_0\sigma(t)v_0\sigma(t')\rangle = v_0^2 e^{-2\gamma|t-t'|}. \tag{1}$$

With the complementary probability $r dt$, the particle undergoes resetting. If this happens, the particle chooses a previous time interval $[t', t' + dt']$ with uniform probability dt'/t, where $0 \leqslant t' \leqslant t$. It then changes the current position x to the position x' it occupied at time t' and also takes the velocity it had at t'. Thus the transition from the state (x, σ, t) to (x', σ', t') occurs with probability $r dt dt'/t$ under this resetting protocol. Figure 1 illustrates these dynamical rules.

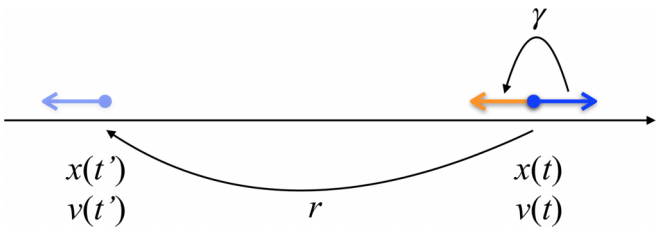

FIG. 1. An active particle (dark blue arrow) moves at constant speed v_0 on the line and stochastically switches direction at rate γ. In addition, the particle can relocate instantaneously to a previously visited location with rate r. In this case, a time $t' \in [0, t)$ is chosen at random uniformly in the past and the particle adopts the position and velocity it had at that time (light blue arrow).

In this model, there are clearly two sources of non-Markovianity. One is the driving noise which has a memory encoded in the autocorrelation function above (which for finite γ is not δ correlated as in the white-noise case). Whereas the complete state of the particle $(x(t), \sigma(t))$ has a Markovian evolution when the motion is driven by the telegraphic noise, the marginal process $x(t)$ is non-Markovian. The second source of non-Markovianity is the resetting moves which depend on the past history of the trajectory. In this case, even the process $(x(t), \sigma(t))$ is non-Markovian. Thus the model is characterized by two timescales: (i) $t_1^* \sim 1/\gamma$, which denotes the typical time between two consecutive switches of the driving noise, and (ii) $t_2^* \sim 1/r$, which denotes the typical time between two consecutive resetting events. The interplay between these two timescales leads to a position distribution $p_r(x, t)$ that is rather rich and nontrivial, as we will illustrate below. We note that a model with the same active dynamics on a line, but subjected to a resetting only to the fixed initial position (with velocity randomized after each reset), was solved exactly in Ref. [19]. The resetting protocol in our model here is thus quite different from that of Ref. [19]. Here, under resetting, both the position and velocity of the particle get reset to the values they had at a previous time, chosen uniformly at random. Consequently, the positions that have been often visited are more likely to be chosen as a resetting point in the future. Actually, under these rules, the probability that the particle chooses a given visited location x' is proportional to the total time it spent at that location.

The rest of the paper is organized as follows. In Sec. II we recall known results on the position distribution of a particle driven by a telegraphic noise only ($r = 0$) and then summarize our main results in the presence of memory ($r > 0$). In Sec. III we present the derivation of the exact Fourier transform $q_r(k, t)$ of the position distribution in the presence of resetting, given by Eq. (9) below. In Sec. IV we derive the exact formula for the variance given by Eq. (13). In Sec. V we derive the large-deviation form, which is summarized in Eq. (15). We summarize and discuss our conclusions in Sec. VI. Appendix A provides a brief summary of the quenched large-deviation principle derived in Ref. [17] by a very different probabilistic approach, along with a comparison with our large-deviation results, which correspond to an annealed case. In Appendix B we give technical details on the small-k expansion of the position distribution up to order 2, from which the variance is obtained.

II. SUMMARY OF KNOWN AND OUR PRESENT RESULTS

In the absence of resetting $r = 0$, the position distribution of a single particle driven by a telegraphic noise has been studied extensively in the past, going back more than 100 years [20,21]. It has repeatedly resurfaced in many different contexts, such as the relativistic chessboard model of Feynman [22], the persistent random-walk model of Kac [23–25], in quantum optics and chemical physics [26], in semiflexible polymer chains in one dimension [27,28], and more recently in the context of active matter [29–37]. Assuming that the particle starts at the origin $x = 0$ with equally likely velocity $\pm v_0$, let $p_0(x, t)$ denote the position distribution at time t, where the subscript 0 refers to zero resetting or $r = 0$. Its Fourier transform has an exact expression at all t [25,33],

$$q_0(k, t) = \int_{-\infty}^{\infty} p_0(x, t) e^{ikx} dx = e^{-\gamma t} \left[\cosh\left(\sqrt{\gamma^2 - v_0^2 k^2}\, t\right) + \frac{\gamma}{\sqrt{\gamma^2 - v_0^2 k^2}} \sinh\left(\sqrt{\gamma^2 - v_0^2 k^2}\, t\right) \right]. \tag{2}$$

By taking derivatives with respect to k at $k = 0$, we can calculate all the moments at all t. For example, the mean is zero by symmetry and the variance $V_0(t) = -\partial_k^2 q_0(k, t)|_{k=0}$ is given by

$$V_0(t) = \frac{v_0^2}{\gamma^2}\left(\gamma t - \frac{1}{2}(1 - e^{-2\gamma t})\right). \tag{3}$$

Since $r = 0$, we have only one timescale $t_1^* \sim 1/\gamma$ in the problem. Indeed, the variance grows differently as a function of t as this timescale is crossed,

$$V_0(t) \simeq \begin{cases} v_0^2 t^2 & \text{for } t \ll 1/\gamma \\ 2D_{\rm eff} t & \text{for } t \gg 1/\gamma, \end{cases} \tag{4}$$

where $D_{\rm eff} = v_0^2/2\gamma$ is the effective diffusion constant. This indicates that for $t \ll 1/\gamma$, where the noise σ is yet to flip, the particle moves ballistically, while for $t \gg 1/\gamma$, the particle undergoes diffusion with an effective diffusion constant $D_{\rm eff}$. Interestingly, in this $r = 0$ case, the Fourier transform in Eq. (2) can be exactly inverted to give [25,27,33]

$$p_0(x, t) = \frac{1}{2} e^{-\gamma t} \left[\delta(x - v_0 t) + \delta(x + v_0 t) + \frac{\gamma}{2v_0}\left(I_0(\rho) + \frac{\gamma t}{\rho} I_1(\rho)\right)\theta(v_0 t - |x|) \right], \tag{5}$$

where $\rho = \frac{\gamma}{v_0}\sqrt{v_0^2 t^2 - x^2}$ and $I_0(z)$ and $I_1(z)$ are modified Bessel functions of the first kind of orders 0 and 1, respectively. Thus, for finite t, the distribution $p_0(x, t)$ is supported over a finite interval $x \in [-v_0 t, v_0 t]$, with two symmetrical δ peaks located at the two edges and a central part that has a Gaussian shape near $x = 0$. As $t \to \infty$, the amplitude of the δ peaks at the two edges vanishes exponentially fast, and for $t \gg 1/\gamma$, the typical fluctuations of $O(\sqrt{t})$ are distributed via the Gaussian form

$$p_0(x, t) \simeq \frac{1}{\sqrt{4\pi D_{\rm eff} t}} e^{-x^2/4D_{\rm eff} t}, \tag{6}$$

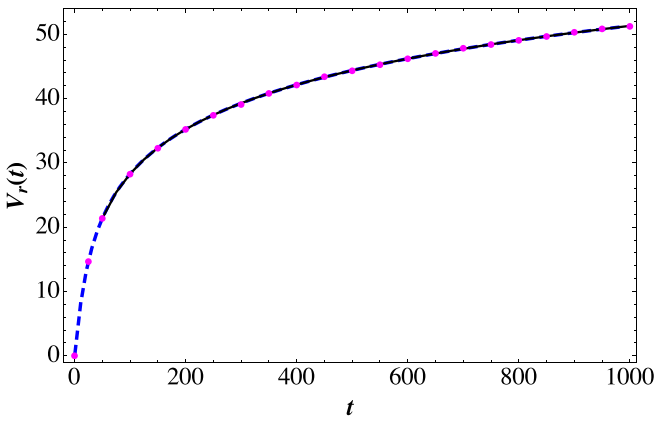

FIG. 2. Variance $V_r(t)$ of the position $x(t)$ as a function of t for $v_0 = 1$, $\gamma = 1$, and $r = 0.1$. The blue dashed line corresponds to the exact result in Eq. (13) and the black solid line to the long-time behavior in Eq. (14). The dots are results of Monte Carlo simulations employing the Gillespie algorithm [40].

where $D_{\rm eff} = \frac{v_0^2}{2\gamma}$. However, the large atypical fluctuations, say, of $O(t)$, are not described by the central Gaussian form. In fact, from the exact distribution in Eq. (5), we find that both the typical and the atypical fluctuations, for large t, are captured by a single large-deviation form [38]

$$p_0(x,t) \sim e^{-\gamma t \Phi_0(x/v_0 t)}, \tag{7}$$

where the rate function $\Phi_0(z)$, supported over $z \in [-1,1]$, is given explicitly by

$$\Phi_0(z) = 1 - \sqrt{1-z^2}, \quad -1 \leqslant z \leqslant 1. \tag{8}$$

In the limit $z \to 0$, i.e., when $|x| \ll v_0 t$, the rate function becomes quadratic $\Phi_0(z) \approx z^2/2$. Substituting this quadratic form in Eq. (7), we recover the Gaussian shape in Eq. (6).

In this paper we provide an exact solution of the position distribution $p_r(x,t)$ when the resetting with rate $r \geqslant 0$ is switched on. Let us first summarize our main results. We assume, as in the $r = 0$ case, that the particle starts at the origin with equally likely velocities $\pm v_0$. We then compute exactly, for all t, the Fourier transform of the position distribution $q_r(k,t) = \int_{-\infty}^{\infty} p_r(x,t) e^{ikx} dx$ and show that it is given by the formula

$$q_r(k,t) = \frac{1}{2}\left[\left(1 - \frac{\gamma}{\sqrt{\gamma^2 - v_0^2 k^2}}\right) f_{\lambda_1(k)}(t) + \left(1 + \frac{\gamma}{\sqrt{\gamma^2 - v_0^2 k^2}}\right) f_{\lambda_2(k)}(t)\right], \tag{9}$$

where

$$\lambda_1(k) = \gamma + \sqrt{\gamma^2 - v_0^2 k^2}, \quad \lambda_2(k) = \gamma - \sqrt{\gamma^2 - v_0^2 k^2}. \tag{10}$$

The function $f_\lambda(t)$ is given explicitly by

$$f_\lambda(t) = M\left(\frac{\lambda}{r+\lambda}, 1, -(r+\lambda)t\right), \tag{11}$$

where $M(a,b,z)$ is the confluent hypergeometric function of the first kind (Kummer's function) that has a simple power series expansion around $z = 0$ [39]:

$$M(a,b,z) = 1 + \frac{a}{b}z + \frac{a(a+1)}{b(b+1)}\frac{z^2}{2!} + \frac{a(a+1)(a+2)}{b(b+1)(b+2)}\frac{z^3}{3!} + \cdots. \tag{12}$$

For $r = 0$, using the identity $M(1,1,z) = e^z$, it is easy to see that Eq. (9) reduces to the expression in Eq. (2).

This exact Fourier transform in Eq. (9), valid for all t, gives access to the moments of $x(t)$. For example, while the mean is zero at all times by symmetry, the variance $V_r(t)$ is given by the explicit expression, valid for all t,

$$V_r(t) = \frac{v_0^2}{2\gamma^2}\left[M\left(\frac{2\gamma}{r+2\gamma}, 1, -(r+2\gamma)t\right) - 1 + \frac{2\gamma}{r}[\ln(rt) + \gamma_E + \Gamma(0,rt)]\right], \tag{13}$$

where $\Gamma(0,z) = \int_z^\infty \frac{e^{-x}}{x} dx$ (for $z > 0$) and $\gamma_E = 0.577\,215\,664\,9\ldots$ is the Euler's constant. A plot of $V_r(t)$ in Eq. (13) as a function of t is provided in Fig. 2, for fixed v_0, γ and r, showing very good agreement with numerical simulations. Again, for $r = 0$, it is easy to check that we recover the result in Eq. (3). For a nonzero r, we have now two timescales $t_1^* \sim 1/\gamma$ and $t_2^* \sim 1/r$. Suppose we have a small resetting rate r so that $t_2^* \gg t_1^*$. The exact variance in Eq. (13) exhibits three different growth regimes: (i) a short-time regime $t \ll t_1^* = 1/\gamma$ where the variance grows quadratically with t, (ii) an intermediate-time regime $1/\gamma \ll t \ll 1/r$ where the variance grows diffusively, and finally (iii) a late-time regime $t \gg 1/r$ where the variance grows extremely slowly as approximately $\ln(rt)$. The precise asymptotic behaviors of the variance are given by

$$V_r(t) \simeq \begin{cases} v_0^2\left[t^2 - \frac{12\gamma+7r}{18}t^3 + O(t^4)\right] & \text{as } t \to 0 \\ \frac{v_0^2}{r\gamma}\left[\ln(rt) + \left(\gamma_E - \frac{r}{2\gamma}\right) + O(t^{-2\gamma/(r+2\gamma)})\right] & \text{as } t \to \infty. \end{cases} \tag{14}$$

The latter expression is also represented in Fig. 2.

Unfortunately, unlike in the $r = 0$ case, we are not able to invert the Fourier transform $q_r(k,t)$ in Eq. (9). Nevertheless, the exact Fourier transform allows us to extract the large-deviation form of $p_r(x,t)$ for large t. We find that it satisfies an anomalous large-deviation form

$$p_r(x,t) \sim (rt)^{-\Psi_r((\sqrt{\gamma r}/v_0)[x/\ln(rt)])} = e^{-\ln(rt)\Psi_r((\sqrt{\gamma r}/v_0)[x/\ln(rt)])}, \tag{15}$$

where the rate function $\Psi_r(z)$ is symmetric $\Psi_r(z) = \Psi_r(-z)$ and can be analytically computed. It has the asymptotic behaviors

$$\Psi_r(z) \simeq \begin{cases} \frac{z^2}{2} & \text{as } z \to 0 \\ \sqrt{2 + \frac{r}{\gamma}}|z| & \text{as } z \to \pm\infty. \end{cases} \tag{16}$$

Substituting the quadratic behavior for small z in Eq. (15), we find that the typical fluctuations of $O(\sqrt{\ln(rt)})$ are described by a Gaussian form

$$p_r(x,t) \sim \exp\left(-\frac{\gamma r x^2}{2v_0^2 \ln(rt)}\right). \tag{17}$$

This result is consistent with late-time behavior of the variance in the second line of Eq. (14). We note that anomalous large-deviation behavior of the type in Eq. (15), where $\ln(rt)$ plays the role of an effective time, has been found also in quite a few unrelated systems such as in persistence problems of Gaussian stationary processes [41,42], in the statistics of the zeros of random Kac-type polynomials [43–45], in models of rainfall records [46], and in certain predator-prey systems [47]. We thus present here analytical expressions where such an anomalous large-deviation form holds with a logarithmic scaling instead of the standard t. Recently, an anomalous large-deviation principle was also proven rigorously by very different methods for a general class of memory models similar to the one considered here and where the time evolution was governed by the law $[\ln(rt)]^\alpha$ with $\alpha > 0$ [17]. The large-deviation principle of [17] corresponds to the quenched case, i.e., when the resetting times are fixed and not averaged over like here. In Appendix A we show that our analytical expression for $\Psi_r(z)$ [see Eq. (75) below] can be rederived by using the general relation of [17].

III. EXACT POSITION DISTRIBUTION

We consider an active self-propelled particle on the line whose position, between resetting events, evolves via $dx/dt = v_0\sigma(t)$, where $\sigma(t) = \pm 1$ is the telegraphic noise that switches between the two states with rate γ. The state of the particle at time t is specified by two degrees of freedom (x,σ), namely, the position and the velocity (in units of v_0). Let us recall the resetting dynamics. At time t, with probability rdt'/t the particle chooses any previous time $t' \leqslant t$ and resets, i.e., the position and velocity get reset to the values taken at t'. Let $p_r(x,\sigma,t)$ denote the probability density that the particle is at position x with velocity σ at time t. To take into account the memory effect, we also need to define the two-point function $p_r(x,\sigma,t;x',\sigma',t')$, which denotes the joint probability density for the particle to be at (x',σ') at time t' and at (x,σ) at t, with $t' \leqslant t$. Clearly, if we integrate the two-point functions over (x',σ') [or alternately over (x,σ)], we recover the marginal one-point probability density

$$\sum_{\sigma'=\pm1} \int_{-\infty}^{\infty} p_r(x,\sigma,t;x',\sigma',t')dx' = p_r(x,\sigma,t) \tag{18a}$$

and similarly

$$\sum_{\sigma=\pm1} \int_{-\infty}^{\infty} p_r(x,\sigma,t;x',\sigma',t')dx = p_r(x',\sigma',t'). \tag{18b}$$

With these ingredients at hand, we can now write down a Fokker-Planck equation for the evolution of the one-point position distributions $p_r(x,\sigma=1,t) \equiv p_r^+(x,t)$ and $p_r(x,\sigma=-1,t) \equiv p_r^-(x,t)$ as

$$\begin{aligned} \partial_t p_r^+(x,t) &= -v_0\partial_x p_r^+(x,t) - \gamma p_r^+(x,t) + \gamma p_r^-(x,t) \\ &\quad - r p_r^+(x,t) + \frac{r}{t}\int_0^t dt' \sum_{\sigma=\pm1}\int_{-\infty}^{\infty} \\ &\quad \times dx' p_r(x',\sigma,t;x,+1,t'), \end{aligned} \tag{19}$$

$$\begin{aligned} \partial_t p_r^-(x,t) &= v_0\partial_x p_r^-(x,t) - \gamma p_r^-(x,t) + \gamma p_r^+(x,t) \\ &\quad - r p_r^-(x,t) + \frac{r}{t}\int_0^t dt' \sum_{\sigma=\pm1}\int_{-\infty}^{\infty} \\ &\quad \times dx' p_r(x',\sigma,t;x,-1,t'). \end{aligned} \tag{20}$$

The first three terms on the right-hand side (rhs) of this pair of equations describe the standard evolution under the self-propelled dynamics. The third term in the first (second) line describes the loss of probability density from position $(x,+1)$ $[(x,-1)]$ at time t due to resetting to other coordinates. The last term on the first (second) line describes the gain in the probability density at $(x,+1)$ $[(x,-1)]$ due to resetting from other positions occupied at time t just before resetting and labeled by (x',σ). If the particle has to reset to $(x,+1)$ $[(x,-1)]$ from (x',σ) at time t, it must have been at $(x,+1)$ $[(x,-1)]$ at a previous time $t' \leqslant t$ and the probability density of this event is simply the two-point function $p_r(x',\sigma,t;x,+1,t')$. Finally, we need to integrate over all (x',σ) from which the particle may arrive at $(x,+1)$ $[(x,-1)]$ by resetting. The reason for the solvability for the one-point position distribution in this model can then traced back to Eq. (18b), which allows us to write a closed pair of equations for the one-point function only, without involving higher-point functions,

$$\begin{aligned} \partial_t p_r^+(x,t) &= -v_0\partial_x p_r^+(x,t) - \gamma p_r^+(x,t) + \gamma p_r^-(x,t) \\ &\quad - r p_r^+(x,t) + \frac{r}{t}\int_0^t dt' p_r^+(x,t'), \end{aligned} \tag{21}$$

$$\begin{aligned} \partial_t p_r^-(x,t) &= v_0\partial_x p_r^-(x,t) - \gamma p_r^-(x,t) + \gamma p_r^+(x,t) \\ &\quad - r p_r^-(x,t) + \frac{r}{t}\int_0^t dt' p_r^-(x,t'). \end{aligned} \tag{22}$$

These two equations start from the initial conditions

$$p_r^+(x,0) = p_r^-(x,0) = \tfrac{1}{2}\delta(x), \tag{23}$$

which corresponds to a particle starting at the origin with equally likely velocities $\pm v_0$. The boundary conditions are $p_r^\pm(x \to \pm\infty, t) = 0$. The full position distribution at time t

is then obtained by summing the two solutions

$$p_r(x,t) = p_r^+(x,t) + p_r^-(x,t). \tag{24}$$

By integrating Eqs. (21) and (22) over x and adding, we can easily check that the total probability $\int_{-\infty}^{\infty} p_r(x,t)dx = 1$ is conserved at all times. Evidently, for $r = 0$, these equations reduce to the standard pair of Fokker-Planck equations studied extensively in the literature [25,33].

To solve the pair of coupled partial differential equations (21) and (22), it turns out to be convenient to work in the Fourier space. We define the pair of Fourier transforms

$$q_r^{\pm}(k,t) = \int_{-\infty}^{\infty} p_r^{\pm}(x,t)e^{ikx}dx. \tag{25}$$

Taking Fourier transforms of Eqs. (21) and (22), we obtain

$$\partial_t q_r^+(k,t) = (iv_0k - \gamma - r)q_r^+(k,t) + \gamma q_r^-(k,t) + \frac{r}{t}\int_0^t q_r^+(k,t')dt', \tag{26}$$

$$\partial_t q_r^-(k,t) = -(iv_0k + \gamma + r)q_r^-(k,t) + \gamma q_r^+(k,t) + \frac{r}{t}\int_0^t q_r^-(k,t')dt'. \tag{27}$$

The initial conditions (23) translate, in the Fourier space, to

$$q_r^+(k,0) = q_r^-(k,0) = \tfrac{1}{2}. \tag{28}$$

Equations (26) and (27) are still coupled and time dependent. To make further progress we make the ansatz

$$q_r^{\pm}(k,t) = f(t,k)u_{\pm}(k). \tag{29}$$

Note that this ansatz is not really a separation of variables since $f(t,k)$ may depend on both t and k. It just assumes that both $q_r^+(k,t)$ and $q_r^+(k,t)$ have the same time dependence through the common shared factor $f(t,k)$. The goal would be to find these functions $f(t,k)$ and $u_{\pm}(k)$. Substituting (29) into the pair of Eqs. (26) and (27) and dividing both sides by $f(t,k)u_{\pm}(k)$ gives

$$\frac{1}{f(t,k)}\partial_t f(t,k) - \frac{r}{tf(t,k)}\int_0^t f(t',k)dt' = (iv_0k - \gamma - r) + \gamma\frac{u_-(k)}{u_+(k)}, \tag{30}$$

$$\frac{1}{f(t,k)}\partial_t f(t,k) - \frac{r}{tf(t,k)}\int_0^t f(t',k)dt' = -(iv_0k + \gamma + r) + \gamma\frac{u_+(k)}{u_-(k)}. \tag{31}$$

It thus follows that the right-hand sides of these two equations cannot be a function of t and they depend only on k. It then follows immediately that the function $f(t,k)$ must satisfy an eigenvaluelike equation

$$\frac{1}{f(t,k)}\partial_t f(t,k) - \frac{r}{tf(t,k)}\int_0^t f(t',k)dt' = -r - \lambda(k), \tag{32}$$

where we defined the eigenvalue $\lambda(k)$ with a shift by r for convenience. From Eqs. (30) and (31) it then follows that the eigenvalue $\lambda(k)$ must satisfy the pair of equations

$$(iv_0k - \gamma) + \gamma\frac{u_-(k)}{u_+(k)} = -\lambda(k), \tag{33}$$

$$-(iv_0k + \gamma) + \gamma\frac{u_+(k)}{u_-(k)} = -\lambda(k). \tag{34}$$

To satisfy both (33) and (34), the eigenvalue $\lambda(k)$ must satisfy

$$[\lambda(k) + iv_0k - \gamma][\lambda(k) - iv_0k - \gamma] - \gamma^2 = 0, \tag{35}$$

which has two roots

$$\lambda_1(k) = \gamma + \sqrt{\gamma^2 - v_0^2k^2}, \quad \lambda_2(k) = \gamma - \sqrt{\gamma^2 - v_0^2k^2}. \tag{36}$$

In addition, for each of these eigenvalues, it follows from Eqs. (33) and (34) that $u_{\pm}(k)$ must also satisfy the relation

$$\frac{u_+(k)}{u_-(k)} = -\frac{\lambda(k) - iv_0k - \gamma}{\gamma} = -\frac{\gamma}{\lambda(k) + iv_0k - \gamma}. \tag{37}$$

Given the eigenvalue $\lambda(k)$, we now need to determine the function $f(t,k)$ from Eq. (32). To solve this equation, we first define

$$F(t,k) = \int_0^t f(t',k)dt', \tag{38}$$

which then satisfies, using (32), the second-order ordinary differential equation (for fixed k)

$$t\frac{d^2F(t,k)}{dt^2} + [r + \lambda(k)]t\frac{dF(t,k)}{dt} - rF(t,k) = 0, \tag{39}$$

subject to the condition

$$F(0,k) = 0, \tag{40}$$

which follows from the definition (38). We now make the substitution

$$F(t,k) = tW(-[r + \lambda(k)]t) \tag{41}$$

in Eq. (39). Then it is straightforward to show that $W(z)$ satisfies the ordinary differential equation

$$zW''(z) + (2 - z)W'(z) - \frac{\lambda(k)}{r + \lambda(k)}W(z) = 0. \tag{42}$$

This is the standard confluent hypergeometric differential equation [39] whose general solution can be written as the linear combination of two independent solutions

$$W(z) = c_1M\left(\frac{\lambda(k)}{r + \lambda(k)}, 2, -z\right) + c_2U\left(\frac{\lambda(k)}{r + \lambda(k)}, 2, -z\right), \tag{43}$$

where c_1 and c_2 are arbitrary constants. Thus, using Eq. (41), the general solution of $F(t,k)$ can be expressed as

$$F(t,k) = c_1tM\left(\frac{\lambda(k)}{r + \lambda(k)}, 2, -[r + \lambda(k)]t\right) + c_2tU\left(\frac{\lambda(k)}{r + \lambda(k)}, 2, -[r + \lambda(k)]t\right). \tag{44}$$

However, this solution must satisfy the constraint $F(0,k)=0$ in (40). Now, using the small argument asymptotics of the two solutions [39]

$$M(a,b,z)\to 1 \quad \text{as } z\to 0, \tag{45}$$

$$U(a,b,z)\to \frac{1}{\Gamma(a)z} \quad \text{as } z\to 0, \tag{46}$$

we find that

$$F(0,k)\to -\frac{c_2}{[r+\lambda(k)]\Gamma\left(\frac{\lambda(k)}{r+\lambda(k)}\right)}. \tag{47}$$

Since $F(0,k)=0$, we must have $c_2=0$. Hence our solution simply reads

$$F(t,k)=c_1 tM\left(\frac{\lambda(k)}{r+\lambda(k)},2,-[r+\lambda(k)]t\right). \tag{48}$$

Taking the derivative with respect to t and using the definition of $M(a,b,z)$ as a power series of z we get

$$f_{\lambda(k)}(t,k)=\frac{dF(t,k)}{dt}=c_1 M\left(\frac{\lambda(k)}{r+\lambda(k)},1,-[r+\lambda(k)]t\right), \tag{49}$$

where we have used the subscript $\lambda(k)$ in $f(t,k)$ to display explicitly its dependence on the eigenvalue $\lambda(k)$.

Thus, given the two eigenvalues $\lambda_1(k)$ and $\lambda_2(k)$ in Eq. (36) and the associated time-dependent parts $f_{\lambda_1(k)}(t,k)$ and $f_{\lambda_2(k)}(t,k)$, we can then write the complete solution [returning to the ansatz (29) and using the relation (37)] as the linear combinations

$$q_r^+(k,t)=u_1^+(k)f_{\lambda_1(k)}(t,k)+u_2^+(k)f_{\lambda_2(k)}(t,k), \tag{50}$$

$$q_r^-(k,t)=-\frac{\lambda_1(k)+iv_0k-\gamma}{\gamma}u_1^+(k)f_{\lambda_1(k)}(t,k) - \frac{\lambda_2(k)+iv_0k-\gamma}{\gamma}u_2^+(k)f_{\lambda_2(k)}(t,k). \tag{51}$$

Note that we can absorb the constant c_1 that appears in $f_{\lambda(k)}(t,k)$ in Eq. (49) in the functions $u_1^+(k)$ and $u_2^+(k)$. In other words, we can set $c_1=1$ in the expression for $f_{\lambda(k)}(t,k)$ in Eq. (49) without any loss of generality. With this convention and using $M(a,b,0)=1$, we then obtain from Eq. (49) that $f_{\lambda(k)}(t=0,k)=1$. The only unknown functions $u_1^+(k)$ and $u_2^+(k)$ in Eqs. (50) and (51) are to be determined from the pair of initial conditions in Eq. (28). Setting $t=0$ in Eqs. (50) and (51) and using $f_{\lambda(k)}(t=0,k)=1$, the initial condition (28) gives the two equations

$$u_1^+(k)+u_2^+(k)=\tfrac{1}{2}, \tag{52}$$

$$-\frac{\lambda_1(k)+iv_0k-\gamma}{\gamma}u_1^+(k)-\frac{\lambda_2(k)+iv_0k-\gamma}{\gamma}u_2^+(k)=\frac{1}{2}. \tag{53}$$

Solving this pair of equations gives

$$u_1^+(k)=-\frac{\gamma-\sqrt{\gamma^2-v_0^2k^2}+iv_0k}{4\sqrt{\gamma^2-v_0^2k^2}}, \tag{54}$$

$$u_2^+(k)=\frac{\gamma+\sqrt{\gamma^2-v_0^2k^2}+iv_0k}{4\sqrt{\gamma^2-v_0^2k^2}}. \tag{55}$$

Substituting the expressions for $u_1^+(k)$, $u_2^+(k)$, and $f_{\lambda(k)}(t,k)$ in Eqs. (50) and (51) then gives us the pair of Fourier transforms $q_r^\pm(k,t)$ explicitly. By gathering the two terms, the Fourier transform of the full position distribution $q_r(k,t)$ is obtained as

$$q_r(k,t)=\int_{-\infty}^{\infty}p_r(x,t)e^{ikx}dx=q_r^+(k,t)+q_r^-(k,t) \tag{56}$$

$$=\frac{1}{2}\left[\left(1-\frac{\gamma}{\sqrt{\gamma^2-v_0^2k^2}}\right)f_{\lambda_1(k)}(t) +\left(1+\frac{\gamma}{\sqrt{\gamma^2-v_0^2k^2}}\right)f_{\lambda_2(k)}(t)\right], \tag{57}$$

where $\lambda_1(k)=\gamma+\sqrt{\gamma^2-v_0^2k^2}$, $\lambda_2(k)=\gamma-\sqrt{\gamma^2-v_0^2k^2}$, and the function $f_{\lambda(k)}(t,k)$ is given in Eq. (49) (with $c_1=1$). This result in Eq. (57) was announced in Eq. (9) in the Introduction.

For later usage, it is also useful to consider the time-integrated position distribution

$$P_r(x,t)=\int_0^t p_r(x,t')dt'. \tag{58}$$

The Fourier transform of $P_r(x,t)$ is given by

$$Q_r(k,t)=\int_{-\infty}^{\infty}P_r(x,t)e^{ikx}dx=\int_0^t q_r(k,t')dt'. \tag{59}$$

Using Eq. (57), we find

$$Q_r(k,t)=\frac{1}{2}\left[\left(1-\frac{\gamma}{\sqrt{\gamma^2-v_0^2k^2}}\right)F_{\lambda_1(k)}(t,k) +\left(1+\frac{\gamma}{\sqrt{\gamma^2-v_0^2k^2}}\right)F_{\lambda_2(k)}(t,k)\right], \tag{60}$$

where again $\lambda_1(k)=\gamma+\sqrt{\gamma^2-v_0^2k^2}$, $\lambda_2(k)=\gamma-\sqrt{\gamma^2-v_0^2k^2}$, and $F_{\lambda(k)}(t,k)$ is given in Eq. (48) (with $c_1=1$), namely,

$$F_{\lambda(k)}(t,k)=tM\left(\frac{\lambda(k)}{r+\lambda(k)},2,-[r+\lambda(k)]t\right), \tag{61}$$

with $M(a,b,z)$ given in Eq. (12).

IV. EXACT COMPUTATION OF THE VARIANCE

From the exact Fourier transform of the position distribution in Eq. (57), we can, in principle, compute all the moments by making a small-k expansion. By symmetry, the mean position is identically zero $\langle x\rangle(t) = 0$ at all times. Thus the variance is given by

$$V_r(t) = \langle x^2\rangle(t) - [\langle x\rangle(t)]^2 = -\frac{d^2 q_r(k,t)}{dk^2}\bigg|_{k=0}. \tag{62}$$

To perform the small-k expansion of $q_r(k,t)$, it turns out to be convenient to work with the time-integrated Fourier transform in Eq. (60). For small k, keeping terms up to $O(k^2)$, we get

$$1 - \frac{\gamma}{\sqrt{\gamma^2 - v_0^2 k^2}} \simeq -\frac{v_0^2 k^2}{2\gamma^2},\quad 1 + \frac{\gamma}{\sqrt{\gamma^2 - v_0^2 k^2}} \simeq 2 + \frac{v_0^2 k^2}{2\gamma^2}. \tag{63}$$

Expanding the eigenvalues in Eq. (36) up to $O(k^2)$, we get

$$\lambda_1(k) \simeq 2\gamma - \frac{v_0^2 k^2}{2\gamma},\quad \lambda_2(k) \simeq \frac{v_0^2 k^2}{2\gamma}. \tag{64}$$

Using these expansions in Eq. (60), we get, after several steps (see Appendix B for details),

$$Q_r(k,t) = t\left\{1 - \frac{v_0^2 k^2}{4\gamma^2}\left[-1 + M\left(\frac{2\gamma}{r+2\gamma}, 2, -(r+2\gamma)t\right) - \gamma t\, {}_2F_2(\{1,1\},\{2,3\},-rt)\right]\right\} + O(k^4). \tag{65}$$

Furthermore, it turns out that the function ${}_2F_2(\{1,1\},\{2,3\},-rt)$ can be expressed in terms of elementary functions as

$${}_2F_2(\{1,1\},\{2,3\},z) = -\frac{2}{z^2}[e^z - 1 - z + \gamma_E z + z\Gamma(0,-z) + z\ln(-z)], \tag{66}$$

where $\Gamma(0,z) = \int_z^\infty e^{-x}dx/x$ for $z > 0$ and γ_E is Euler's constant.

Deriving Eq. (65) twice with respect to k and setting $k = 0$ gives the time-integrated variance

$$\int_0^t V_r(t')dt' = \frac{v_0^2}{2\gamma^2}\left[-t + tM\left(\frac{2\gamma}{r+2\gamma}, 2, -(r+2\gamma)t\right) + \frac{2\gamma}{r^2}g(rt)\right], \tag{67}$$

where

$$g(y) = 1 - e^{-y} + y\ln(y) + y\int_y^\infty \frac{e^{-x}}{x}dx - (1-\gamma_E)y. \tag{68}$$

Finally, taking a derivative with respect to t gives our final exact expression for the variance, valid for all t and given by Eq. (13) in the Introduction. In the limit $r \to 0$, it is easy to show, using $M(1,2,z) = (e^z - 1)/z$, that Eq. (13) reduces to the known result in Eq. (3). One can also derive the asymptotic behaviors of $V_r(t)$ for small and large t, as shown in Eq. (14).

V. LARGE-DEVIATION FORM AT LATE TIMES

While we cannot invert the Fourier transform $q_r(k,t)$ in Eq. (57) to obtain the position distribution $p_r(x,t)$ in real space for all t, we show in this section that we can make progress at large times. We show below that $p_r(x,t)$ indeed admits an anomalous large-deviation form as in Eq. (15). For large t, the asymptotic behavior of the Fourier transform $q_r(k,t)$ in Eq. (57) can be derived by using the following property of $M(a,b,z)$ [39]:

$$M(a,b,-z) \simeq \frac{\Gamma(b)}{\Gamma(b-a)}z^{-a} \quad \text{as } z \to \infty. \tag{69}$$

Using this result in Eq. (57), we find that for $t \gg 1/(r+2\gamma)$ (and fixed k) the leading term of the Fourier transform $q_r(k,t)$ decays as (up to a prefactor independent of time)

$$q_r(k,t) \sim \left[\left(1 + \frac{\lambda_2(k)}{r}\right)rt\right]^{-\lambda_2(k)/[r+\lambda_2(k)]} \sim (rt)^{-\lambda_2(k)/[r+\lambda_2(k)]} = e^{-\lambda_2(k)/[r+\lambda_2(k)]\ln(rt)}. \tag{70}$$

The contribution coming from $\lambda_1(k)$ is subleading since $\lambda_1(k) > \lambda_2(k)$ in Eq. (36). Inverting formally the Fourier transform (70) and using $\lambda_2(k) = \gamma - \sqrt{\gamma^2 - v_0^2 k^2}$, we get, to leading order for large t,

$$p_r(x,t) = \int_{-\infty}^\infty \frac{dk}{2\pi}e^{-ikx}q_r(k,t) \sim \int_{-\infty}^\infty \frac{dk}{2\pi} \times \exp\left(-ikx - \frac{\gamma - \sqrt{\gamma^2 - v_0^2k^2}}{r + \gamma - \sqrt{\gamma^2 - v_0^2k^2}}\ln(rt)\right). \tag{71}$$

It is now convenient to make a change of variable $ikv_0/\sqrt{\gamma r} = q$ (Wick's rotation) and rewrite the k integral as a Bromwich integral in the complex q plane

$$p_r(x,t) \sim \frac{\sqrt{\gamma r}}{v_0}\int_\Gamma \frac{dq}{2\pi i} \times \exp\left[-\ln(rt)\left(1 + qz - \frac{R}{1 + R - \sqrt{1+Rq^2}}\right)\right], \tag{72}$$

with $R = \frac{r}{\gamma}$. The contour Γ runs vertically in the complex q plane without a real shift and we have defined

$$z = \frac{\sqrt{\gamma r}x}{v_0\ln(rt)}. \tag{73}$$

Let us first remark that $p_r(x,t)$ in Eq. (71) is clearly symmetric in x, or equivalently in Eq. (72) as a function of the scaled variable z. Hence, without any loss of generality, we will just consider the case $z \geqslant 0$.

Now, for large t, we can evaluate the integral in Eq. (72) by the saddle-point method. This gives the desired large-deviation form

$$p_r(x,t) \sim \exp[-\ln(rt)\Psi_r(z)], \tag{74}$$

where $z = \frac{\sqrt{\gamma r}x}{v_0\ln(rt)}$ and the rate function $\Psi_r(z)$ is symmetric around $z = 0$, i.e., $\Psi_r(-z) = \Psi_r(z)$. For $z \geqslant 0$, the rate

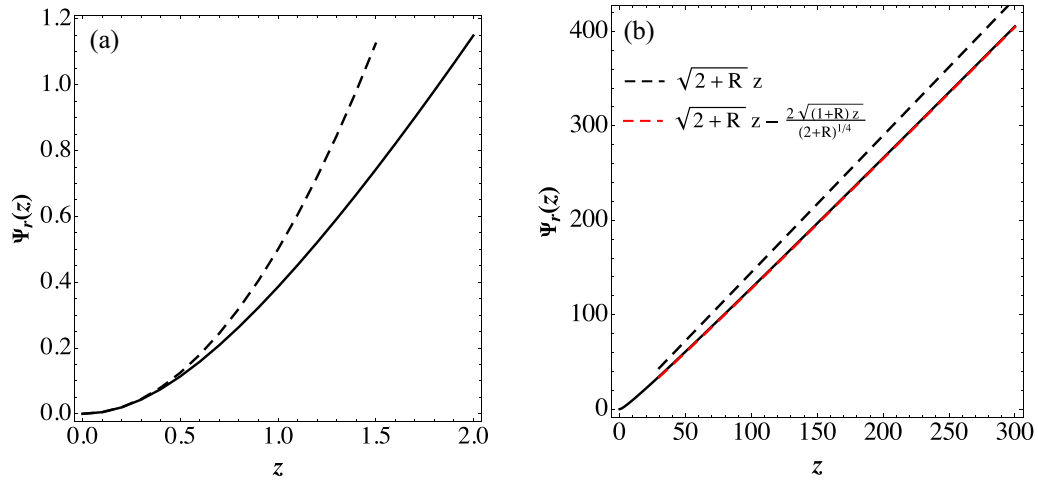

FIG. 3. (a) Analytical rate function $\Psi_r(z)$ in Eq. (75) plotted against z (solid line) for fixed $r = 0.1$ and $\gamma = 1$ (or $R = r/\gamma = 0.1$); the quadratic behavior at small z in Eq. (82) is displayed with a dashed line. (b) Same rate function at large z (solid line), with the leading asymptotic form in Eq. (82) shown as a black dashed line. The red dashed line represents the leading term plus the first subleading correction.

function $\Psi_r(z)$ is obtained from the following maximization, i.e., the saddle-point analysis of Eq. (72):

$$\Psi_r(z) = \sup_{0\leqslant q\leqslant q_{\max}} \left(1 + qz - \frac{R}{1+R-\sqrt{1+Rq^2}}\right). \quad (75)$$

Note that in the maximization over q above, the range of q is limited over $q \in [0, q_{\max}]$, where $q_{\max}$ is given by

$$1 + R - \sqrt{1 + Rq_{\max}^2} = 0 \quad \text{or} \quad q_{\max} = \sqrt{R+2}. \quad (76)$$

To compute the rate function $\Psi_r(z)$, we proceed as follows. Let us first define

$$S(q, z) = 1 + qz - \frac{R}{1+R-\sqrt{1+Rq^2}}. \quad (77)$$

Deriving with respect to q and setting it to zero, i.e., $\partial_q S(q, z) = 0$, gives $q = q^*(z)$, where

$$z = \frac{q^* R^2}{\sqrt{1+R(q^*)^2}[1+R-\sqrt{1+R(q^*)^2}]}. \quad (78)$$

Now evaluating the action $S(q, z)$ at $q = q^*$ gives the rate function

$$\Psi_r(z) = S(q^*(z), z) = 1 - \frac{R}{1+R-\sqrt{1+R(q^*(z))^2}} + q^*(z)z, \quad (79)$$

where z depends on q^* through Eq. (78). We need to eliminate q^* from Eqs. (79) and (78) to express $\Psi_r(z)$ as a function of z. This can be done using a parametric plot in *Mathematica* that lets us plot $\Psi_r(z)$ as a function of z in Fig. 3(a). Note that we have only plotted $\Psi_r(z)$ for $z \geqslant 0$. For the negative argument, we would simply use the symmetry $\Psi_r(-z) = \Psi_r(z)$.

We can also derive the asymptotic behaviors of $\Psi_r(z)$ as $z \to 0$ and $z \to \infty$. To derive these behaviors, let us first express $\Psi_r(z)$ in a convenient form. Indeed, by taking a total derivative of $\Psi_r(z)$ in Eq. (79), we get

$$\frac{d\Psi_r(z)}{dz} = q^*(z) + \partial_q S(q, z)\Big|_{q=q^*(z)} \frac{dq^*(z)}{dz} = q^*(z), \quad (80)$$

where the last equality holds because the second term on the rhs vanishes, as $\partial_q S(q, z) = 0$ at the saddle point $q = q^*(z)$. Now integrating Eq. (80) with respect to z gives the exact identity (assuming $z \geqslant 0$)

$$\Psi_r(z) = \int_0^z q^*(z')dz', \quad (81)$$

where we used the fact that $\Psi_r(z = 0) = 0$. Thus, we need to first solve $q^*(z)$ implicitly as a function of z from Eq. (78) and then use it in Eq. (81) to derive $\Psi_r(z)$. This gives us access to the asymptotic behaviors of $\Psi_r(z)$. For example, when $z \to 0$, we get from Eq. (78) that $q^*(z) \simeq z$. Hence, from Eq. (81) we get $\Psi_r(z) \simeq z^2/2$. In contrast, when $z \to \infty$, we expect $q^* \to q_{\max} = \sqrt{2+R}$ defined in Eq. (76). Hence, from Eq. (81) we obtain a linear growth $\Psi_r(z) = \sqrt{R+2}z$ for large z. By symmetry, it behaves as $\Psi_r(z) = \sqrt{R+2}|z|$ as $z \to -\infty$. In summary, using $R = r/\gamma$, the two asymptotic limits are given by

$$\Psi_r(z) \simeq \begin{cases} \frac{z^2}{2} & \text{as } z \to 0 \\ \sqrt{2+\frac{r}{\gamma}}|z| & \text{as } z \to \pm\infty. \end{cases} \quad (82)$$

The quadratic form and the crossover to linear behavior as z increases can be seen in Fig. 3(a). Figure 3(b) shows that the rate function at large z tends to the linear form in Eq. (82). We have also represented this asymptotic behavior plus the first subleading correction, of order $|z|^{1/2}$, giving very good agreement with the actual $\Psi_r(z)$. We have not attempted to perform a comparison of the large-deviation function with numerical simulations because of the very slow convergence toward the large-t asymptotic limit. As already noted in Ref. [1], the convergence to the Gaussian central part is extremely slow, as the leading corrections are of the order of $1/\ln(t)$ and still not negligible at the times that can be accessed numerically.

The two asymptotic limits of the rate function $\Psi_r(z)$ have interesting physical implications. For $z \to 0$, substituting the quadratic behavior of $\Psi_r(z)$ in the large-deviation form in Eq. (74), we get

$$p_r(x,t) \sim \exp\left(-\frac{\gamma r x^2}{2v_0^2 \ln(rt)}\right) \quad \text{for } |x| \ll \ln(rt), \tag{83}$$

which shows that the typical fluctuations of $O(\sqrt{\ln(rt)})$ around the mean are Gaussianly distributed. Moreover, the variance $v_0^2 \ln(rt)/\gamma r$ matches perfectly with the leading asymptotic growth of the variance in Eq. (14). Furthermore, using $D_{\rm eff} = v_0^2/2\gamma$, we recover, at late times, the Gaussian behavior with variance $(2D_{\rm eff}/r)\ln(rt)$ as in ordinary diffusion with the same memory-dependent resetting [1,13]. This is expected since at very late times the active dynamics is known to effectively behave as a standard diffusion with an effective diffusion constant $D_{\rm eff} = v_0^2/2\gamma$.

In the opposite limit $|z| \to \infty$, we get, by substituting the linear behavior (82) into the large-deviation form (74),

$$p_r(x,t) \sim \exp\left(-\frac{\sqrt{r(r+2\gamma)}}{v_0}|x|\right) \quad \text{for } |x| \gg \ln(rt). \tag{84}$$

This result may, at first glance, look surprising because it says that very far away from the center, i.e., for $|x| \gg \ln(rt)$, the distribution actually becomes time independent at late times. However, this is what one would expect in hindsight. At late times, the particle is essentially concentrated in a core region around the origin of width $\sqrt{\ln(rt)}$. Seen from very far away from the core, the dynamics essentially reduces to an active particle that is reset effectively to the origin. This later problem was studied in Ref. [19] and the authors demonstrated that the position distribution approaches a stationary form at late times which happens to exactly coincide with Eq. (84). Thus it is quite natural that $p_r(x,t)$ in our problem, for $|x| \gg \ln(rt)$, becomes stationary as shown by Eq. (84). In Appendix A we show that the results of this section are consistent with the recent findings of Ref. [17].

VI. CONCLUSION

We have studied an active diffusion model with memory in one spatial dimension, in which a self-propelled particle moves at constant speed v_0 and switches direction stochastically at rate γ. Memory effects are implemented through a protocol where the particle interrupts its active motion and resets at rate r to positions and velocities that were occupied at previous times. More specifically, during a time interval $[t, t+dt]$, with probability rdt the particle chooses a time t' in the past, uniformly distributed in $[0,t]$, and takes the position and velocity it had at time t', before continuing its active motion from there. This model extends previous studies that considered random walks or Brownian particles with similar resetting protocols [1,11–13]. The case studied here also differs significantly from the same active process in which resetting occurs to a unique position, e.g., the starting position [19], due to the fact that it lacks a steady state. The memory rule makes the particle return more often to positions frequently occupied (typically near its starting position), generating a diffusive process in which the variance of the position grows very slowly with time, but without being arrested asymptotically.

We have calculated exactly the distribution of the position of the particle in Fourier space, extending the results of Ref. [13] for Brownian motion. While we were not able to invert this Fourier transform, we used it to calculate exactly the full time dependence of the variance of the position. The interplay between activity and memory leads to a variance growing as t^2 at short times and as $\ln(rt)$ as long times, this latter regime being a fingerprint of preferential visit models. The knowledge of the position distribution, whose central part becomes Gaussian at long times, allowed us to derive a large-deviation principle and to study the rate function explicitly for this type of process. At distances much larger than a typical scale $\ln(rt)$, the distribution of the position becomes exponential, independent of time, and coincides with the nonequilibrium steady state produced by resetting an active particle to its starting position only.

This problem could be generalized in several directions in the future, for instance, to other protocols such as those involving periodic resetting. The results recently derived in Ref. [17] for large deviations could be applied to this case and many others. Systems of many independent particles become correlated over time when subject to simultaneous resetting [48,49]. How correlations are built though resetting in preferential revisit models is also a question that deserves further study.

ACKNOWLEDGMENTS

S.N.M. is grateful for the hospitality of KITP, Santa Barabra where this work was initiated, supported in part by the National Science Foundation under Grant No. NSF PHY-1748958. D.B. acknowledges support from CONACYT (Mexico) project Ciencia de Frontera through Grant No. 2019/10872.

APPENDIX A: QUENCHED LARGE-DEVIATION PRINCIPLE FOR BROWNIAN AND ACTIVE PARTICLES WITH MEMORY

We show that our results on large deviations, in particular the expression (75) of the rate function, can be derived by an alternative method using a recent theorem of Boci and Mailler valid for a more general class of processes with preferential revisits [17]. We first recall briefly their main results. Let $z(t)$ be a Markov process and $\boldsymbol{L} = \{L_i\}_{i\in\mathbb{N}}$ an infinite set of independent and identically distributed positive random variables, each distributed via $\phi(L)$. The L_i's represent the time intervals between successive resetting events. During each such interval the position of the walker $x(t)$ evolves freely according to the process $z(t)$. When the nth resetting occurs (at time $t_n = \sum_{i=1}^n L_i$), the walker randomly chooses a time in the past $t' \in [0, t_n]$ with a normalized probability density $\mu(t')/\int_0^{t_n} dt\, \mu(t)$, where μ is a given function, and relocates to the position it occupied at that time, i.e., $x(t_n) = x(t')$. From there, x continues to evolve as z until the next resetting at time t_{n+1}. While we take a uniform kernel $\mu(t') = 1$, Boci and

Mailler considered a more general form

$$\mu(t') = \frac{\alpha}{t'}(\ln t')^{\alpha-1} e^{\beta(\ln t')^{\alpha}}, \tag{A1}$$

which reduces to the uniform case when $\alpha = \beta = 1$.

The next goal is to find a large-deviation principle for the position $x(t)$, given that a large-deviation principle exists for the underlying free Markov process $z(t)$ between two resettings. The prescription of Boci and Mailler for computing this large-deviation principle proceeds via three steps (here we simplify the notation of Ref. [17] to adapt to the language of physicists).

(i) One first assumes that the free Markov process $z(t)$ admits a large-deviation principle, i.e., there exists a function $\Lambda(\zeta)$ such that

$$\lim_{t\to\infty} \frac{1}{t} \ln\langle e^{\zeta z(t)}\rangle = \Lambda(\zeta) \tag{A2}$$

for all ζ and with $z(t=0)$ fixed. This simply means that, to leading order for large t,

$$\langle e^{\zeta z(t)}\rangle \sim \exp[t\,\Lambda(\zeta)]. \tag{A3}$$

(ii) The next step is to compute the generating function $g(\xi)$ for all ξ,

$$g(\xi) \equiv \frac{\langle e^{\xi L} - 1 - \xi L\rangle}{\xi \langle L\rangle} = \frac{\int_0^\infty (e^{\xi L} - 1 - \xi L)\phi(L)dL}{\xi \int_0^\infty L\phi(L)dL}, \tag{A4}$$

where we recall that $\phi(L)$ is the distribution of the interval L between two successive resets.

(iii) Knowing the two functions $\Lambda(\zeta)$ and $g(\xi)$ from above, the final step consists in computing the Legendre transform

$$\Psi(w) = \sup_y [wy - g(\Lambda(y))]. \tag{A5}$$

Once $\Psi(w)$ is computed, the Boci-Mailler theorem states that under rather mild conditions the position $x(t)$ satisfies a quenched large-deviation principle, i.e., conditioned on the L_i's. For all $w > 0$, this principle can be written as

$$\lim_{t\to\infty} \frac{\ln\{\text{Prob}[|x(t)| \geqslant w s(t)|\boldsymbol{L}]\}}{s(t)} = -\inf_{y\geqslant w} \Psi(y) = -\Psi(w), \tag{A6}$$

where the last equality assumes that $\Psi(y)$ is a monotonically increasing function of y. The scaling factor $s(t)$ is given by

$$s(t) = (\ln t)^{\alpha} \quad \text{if } \beta \neq 0. \tag{A7}$$

In the language of physicists, the statement in Eq. (A6) simply means that to leading order in large t, the cumulative position distribution behaves as

$$\text{Prob}[|x(t)| \geqslant X] \sim \exp\left[-(\ln t)^{\alpha}\Psi\left(\frac{X}{(\ln t)^{\alpha}}\right)\right], \tag{A8}$$

where the rate function $\Psi(w)$ is computed from Eq. (A5). For the uniform memory kernel where $\alpha = 1$ and $\beta = 1$, Eq. (A8) takes precisely our large-deviation form in Eq. (74).

The results in Eqs. (A8) and (A5) were derived in Ref. [17] by a very different probabilistic method, namely, a mapping of the memory-induced resetting random walk to a weighted random recursive tree. This is a quenched principle in the sense that the averages are not taken over $\boldsymbol{L}$. The authors of Ref. [17] nevertheless believe that the same principle should hold in the more difficult annealed case, provided $\phi(L)$ decays to 0 fast enough at large L. Below we apply this general prescription to compute the large-deviation principle in two simple cases. In both cases, we assume

$$\phi(L) = re^{-rL} \quad \text{for } L \geqslant 0, \tag{A9}$$

where r represents the resetting rate.

(i) When the underlying free process $z(t)$ is a standard Brownian motion in one dimension. We first compute $\Lambda(\zeta)$ in Eq. (A2). This is easy since

$$\langle e^{\zeta z(t)}\rangle = \int_{-\infty}^{\infty} \frac{dz}{\sqrt{4\pi Dt}} e^{\zeta z - z^2/4Dt} = e^{Dt\zeta^2}, \tag{A10}$$

implying from Eq. (A2) that

$$\Lambda(\zeta) = D\zeta^2. \tag{A11}$$

Next, substituting $\phi(L)$ from Eq. (A9) in (A4), it is easy to see that

$$g(\xi) = \begin{cases} \frac{\xi}{r-\xi} & \text{if } \xi < r \\ \infty & \text{if } \xi \geqslant r. \end{cases} \tag{A12}$$

We use Eq. (A5) with the functions $\Lambda(\zeta)$ and $g(\xi)$ explicitly given by Eqs. (A11) and (A12), respectively, and obtain, for the Brownian motion with memory-induced resetting,

$$\Psi_{\text{BM}}(w) = \sup_{0<y<\sqrt{r/D}} \left(wy - \frac{y^2}{r/D - y^2}\right) \quad \text{for } w \geqslant 0. \tag{A13}$$

The rate function $\Psi_{\text{BM}}(w)$ is symmetric in w; hence it suffices just to consider $w \geqslant 0$. We note that the function inside the supremum in (A13) diverges at $y = \sqrt{r/D}$, thus making the allowed interval for y bounded. This is similar to the situation we encountered in Eq. (75) before. It is a consequence of Eq. (A12) and of the fact that $\phi(L)$ does not decay faster than an exponential at large L.

The above result for the Brownian case can also be derived from our active particle calculation by setting $r \ll \gamma$, i.e., by expanding Eq. (75) at first order in R. Then, recalling that $D_{\text{eff}} = v_0^2/2\gamma$ and $z = \sqrt{r/2D_{\text{eff}}}(x/\ln t)$ in the notation of Sec. V, we make the change of variables $x/\ln t \to w$ and $\sqrt{r/2D_{\text{eff}}}q \to y$ in Eq. (75) and actually recover Eq. (A13) with $D = D_{\text{eff}}$.

Although the maximization of Eq. (A13) cannot be carried out explicitly, we can study the behavior of $\Psi_{\text{BM}}(w)$ at small and large w, in the same way as in Sec. V. It is easy to show that $\Psi_{\text{BM}}(w)$ has the asymptotic behaviors

$$\Psi_{\text{BM}}(w) \simeq \begin{cases} \frac{r}{4D}w^2 & \text{as } |w| \to 0 \\ \sqrt{\frac{r}{D}}|w| & \text{as } |w| \to \infty. \end{cases} \tag{A14}$$

Consequently, Eq. (A8) gives

$$\text{Prob}[|x(t)| > X] \propto \begin{cases} \exp\left(-\frac{X^2}{\frac{4D}{r}(\ln t)^{\alpha}}\right) & \text{as} \quad X \ll (\ln t)^{\alpha} \\ \exp(-\sqrt{\frac{r}{D}}X) & \text{as} \quad X \gg (\ln t)^{\alpha}. \end{cases} \tag{A15}$$

This result agrees with Eq. (83) with D in (A15) replaced by $D_{\rm eff} = v_0^2/2\gamma$ and $\alpha = 1$, while the large deviations are again independent of time at large X and coincide with the nonequilibrium steady state of a Brownian particle under stochastic resetting to the origin only [2].

(ii) When the underlying process $z(t)$ corresponds to a free run-and-tumble particle in one dimension. Here $z(t)$ is the position of the active particle driven by the telegraphic noise. Although this process is non-Markov, we may still try to apply the general prescriptions in Eqs. (A3)–(A6) to this case.[1] To compute $\Lambda(\zeta)$ for the active particle, we start from the general relation

$$\langle e^{\zeta z(t)}\rangle = \int_{-\infty}^{\infty} dz\, e^{\zeta z} P(z,t) \sim e^{\Lambda(\zeta) t}, \tag{A16}$$

where $P(z,t)$ is the position distribution of the active particle at time t. As the exact expression for $P(z,t)$ is not so simple [see Eq. (5)], we rather take the Laplace transform of Eq. (A16) with respect to t and get

$$\int_{-\infty}^{\infty} dz\, e^{\zeta z} \tilde{P}(z,s) \sim \frac{1}{s-\Lambda(\zeta)}, \tag{A17}$$

where $s > \Lambda(\zeta)$ and $\tilde{P}(z,s) = \int_0^\infty dt\, e^{-st} P(z,t)$. Therefore, $\Lambda(\zeta)$ is the largest real pole of the integral on the left-hand side of Eq. (A17). This integral can be calculated from the known expression for $\tilde{P}(z,s)$ (see, e.g., [19]), given explicitly by

$$\tilde{P}(z,s) = \frac{\lambda(s)}{2s}\, e^{-\lambda(s)|z|}, \tag{A18}$$

with $\lambda(s) = \sqrt{s(s+2\gamma)}/v_0$. We then obtain

$$\int_{-\infty}^{\infty} dz\, e^{\zeta z} \tilde{P}(z,s) = \frac{\lambda(s)}{2s}\left(\frac{1}{\lambda(s)-\zeta} + \frac{1}{\lambda(s)+\zeta}\right). \tag{A19}$$

Assuming $\zeta > 0$ without loss of generality (since the active particle process is symmetric), a pole is contained in the first term on the rhs of Eq. (A19),

$$\frac{1}{\lambda(s)-\zeta} \simeq \frac{1}{\lambda'(s^*)(s-s^*)}, \tag{A20}$$

where s^* is the largest root of the equation $\lambda(s) - \zeta = 0$. Identifying s^* with $\Lambda(\zeta)$, we deduce from Eq. (A18)

$$\Lambda(\zeta) = -\gamma + \sqrt{\gamma^2 + v_0^2\zeta^2}. \tag{A21}$$

Inserting this expression in Eq. (A5) with $g(\xi)$ given by Eq. (A12), the rate function becomes

$$\Psi_{\rm active}(w) = \sup_{0<y<y_{\rm max}} \left(wy - \frac{\sqrt{1+\frac{v_0^2}{\gamma^2}y^2} - 1}{1 + R - \sqrt{1+\frac{v_0^2}{\gamma^2}y^2}} \right), \tag{A22}$$

with $R = \frac{r}{\gamma}$. By making the same changes of variable as in the Brownian motion case above, we see that Eq. (A22) is equivalent to Eq. (75).

[1] We may consider the active process as a two-dimensional Markov process $\boldsymbol{Z}(t) = (z(t), \sigma(t))$. The Boci-Mailler theorem applies with $\langle e^{\boldsymbol{\xi}\cdot\boldsymbol{Z}(t)}\rangle$ in Eq. (A2) with $\boldsymbol{\zeta} = (\zeta_z, \zeta_\sigma)$. In the analysis, we then set $\xi_\sigma = 0$.

APPENDIX B: SMALL-k EXPANSION OF $Q_r(k,t)$ UP TO ORDER 2

Substituting the small-k expansions (63) and (64) in the expression (60) of $Q_r(k,t)$, we get

$$Q_r(k,t) \simeq \frac{t}{2}\Bigg[-\frac{v_0^2k^2}{2\gamma^2} M\left(\frac{\lambda_1(k)}{r+\lambda_1(k)}, 2, -[r+\lambda_1(k)]t\right) + \left(2 + \frac{v_0^2k^2}{2\gamma^2}\right) M\left(\frac{\lambda_2(k)}{r+\lambda_2(k)}, 2, -[r+\lambda_2(k)]t\right)\Bigg]. \tag{B1}$$

Since we are interested in the expansion only up to $O(k^2)$ for small k, we can now put $k = 0$ in the arguments of the function M in the first term on the rhs of Eq. (B1), i.e.,

$$M\left(\frac{\lambda_1(k)}{r+\lambda_1(k)}, 2, -[r+\lambda_1(k)]t\right) \simeq M\left(\frac{2\gamma}{r+2\gamma}, 2, -(r+2\gamma)t\right). \tag{B2}$$

For the second term on the rhs of Eq. (B1), we need to expand the arguments of M for small k. Using Eq. (64), we get

$$\frac{\lambda_2(k)}{r+\lambda_2(k)} \simeq \frac{v_0^2k^2}{2\gamma r}, \quad r+\lambda_2(k) \simeq r + \frac{v_0^2k^2}{2\gamma}. \tag{B3}$$

Thus the M function in the second term on the rhs in Eq. (B1) reduces to

$$M\left(\frac{\lambda_2(k)}{r+\lambda_2(k)}, 2, -[r+\lambda_2(k)]t\right) \simeq M\left(\frac{v_0^2k^2}{2\gamma r}, 2, -\left(r+\frac{v_0^2k^2}{2\gamma}\right)t\right). \tag{B4}$$

We now need to expand this function for small k up to $O(k^2)$. This is a bit tricky. We first expand the third argument of M in Eq. (B4) and get

$$M\left(\frac{\lambda_2(k)}{r+\lambda_2(k)}, 2, -[r+\lambda_2(k)]t\right) \simeq M\left(\frac{v_0^2k^2}{2\gamma r}, 2, -rt\right) - \frac{v_0^2k^2}{2\gamma} t\, \partial_z M\left(\frac{v_0^2k^2}{2\gamma r}, 2, z\right)\Big|_{z=-rt}. \tag{B5}$$

Using the identity $\partial_z M(a,b,z) = (a/b)M(a+1,b+1,z)$, we see that the second term in Eq. (B5) is of $O(k^4)$ for small k. Hence we can neglect the second term, and up to $O(k^2)$

we get

$$M\left(\frac{\lambda_2(k)}{r+\lambda_2(k)}, 2, -[r+\lambda_2(k)]t\right) \simeq M\left(\frac{v_0^2k^2}{2\gamma r}, 2, -rt\right). \tag{B6}$$

Now we need to expand the rhs of Eq. (B6) for small k. For this, it is useful to use the small-a expansion of $M(a,b,z)$,

$$M(a,b,z) = 1 + \frac{a}{b} z\, {}_2F_2(\{1,1\},\{2,1+b\},z) + O(a^2), \tag{B7}$$

where ${}_2F_2$ is the generalized hypergeometric function. Hence, from Eq. (B6) we get

$$M\left(\frac{\lambda_2(k)}{r+\lambda_2(k)}, 2, -[r+\lambda_2(k)]t\right) \simeq 1 - \frac{v_0^2k^2}{4\gamma} t\, {}_2F_2(\{1,1\},\{2,3\},-rt). \tag{B8}$$

Collecting all these expansions together into Eq. (B1), we finally get the small-k expansion of $Q_r(k,t)$ given by Eq. (65).

[1] D. Boyer and C. Solis-Salas, Random walks with preferential relocations to places visited in the past and their application to biology, Phys. Rev. Lett. **112**, 240601 (2014).

[2] M. R. Evans and S. N. Majumdar, Diffusion with stochastic resetting, Phys. Rev. Lett. **106**, 160601 (2011).

[3] M. R. Evans, S. N. Majumdar, and G. Schehr, Stochastic resetting and applications, J. Phys. A: Math. Theor. **53**, 193001 (2020).

[4] L. Börger, B. D. Dalziel, and J. M. Fryxell, Are there general mechanisms of animal home range behaviour? A review and prospects for future research, Ecol. Lett. **11**, 637 (2008).

[5] J. M. Fryxell, M. Hazell, L. Börger, B. D. Dalziel, D. T. Haydon, J. M. Morales, T. McIntosh, and R. C. Rosatte, Multiple movement modes by large herbivores at multiple spatiotemporal scales, Proc. Natl. Acad. Sci. USA **105**, 19114 (2008).

[6] B. Van Moorter, D. Visscher, S. Benhamou, L. Börger, M. S. Boyce, and J.-M. Gaillard, Memory keeps you at home: A mechanistic model for home range emergence, Oikos **118**, 641 (2009).

[7] W. F. Fagan, M. A. Lewis, M. Auger-Méthé, T. Avgar, S. Benhamou, G. Breed, L. LaDage, U. E. Schlägel, W.-w. Tang, Y. P. Papastamatiou, J. Forester, and T. Mueller, Spatial memory and animal movement, Ecol. Lett. **16**, 1316 (2013).

[8] J. Merkle, D. Fortin, and J. M. Morales, A memory-based foraging tactic reveals an adaptive mechanism for restricted space use, Ecol. Lett. **17**, 924 (2014).

[9] A. Falcón-Cortés, D. Boyer, E. Merrill, J. L. Frair, and J. M. Morales, Hierarchical, memory-based movement models for translocated elk (*Cervus canadensis*), Front. Ecol. Evol. **9**, 702925 (2021).

[10] W. F. Fagan, F. McBride, and L. Koralov, Reinforced diffusions as models of memory-mediated animal movement, J. R. Soc. Interface **20**, 20220700 (2023).

[11] D. Boyer and J. C. R. Romo-Cruz, Solvable random walk model with memory and its relations with Markovian models of anomalous diffusion, Phys. Rev. E **90**, 042136 (2014).

[12] D. Boyer and I. Pineda, Slow Lévy flights, Phys. Rev. E **93**, 022103 (2016).

[13] D. Boyer, M. R. Evans, and S. N. Majumdar, Long time scaling behaviour for diffusion with resetting and memory, J. Stat. Mech. (2017) 023208.

[14] A. Falcón-Cortés, D. Boyer, L. Giuggioli, and S. N. Majumdar, Localization transition induced by learning in random searches, Phys. Rev. Lett. **119**, 140603 (2017).

[15] D. Boyer, A. Falcon-Cortes, L. Giuggioli, and S. N. Majumdar, Anderson-like localization transition of random walks with resetting, J. Stat. Mech. (2019) 053204.

[16] C. Mailler and G. Uribe-Bravo, Random walks with preferential relocations and fading memory: a study through random recursive trees, J. Stat. Mech. (2019) 093206.

[17] E.-S. Boci and C. Mailler, Large deviation principle for a stochastic process with random reinforced relocations, J. Stat. Mech. (2023) 083206.

[18] E. A. Codling, M. J. Plank, and S. Benhamou, Random walk models in biology, J. R. Soc. Interface **5**, 813 (2008).

[19] M. R. Evans and S. N. Majumdar, Run and tumble particle under resetting: A renewal approach, J. Phys. A: Math. Theor. **51**, 475003 (2018).

[20] R. Fürth, *Schwankungserscheinungen in der Physik* (Sammlung Vieweg, Braunschweig, 1920).

[21] G. I. Taylor, Diffusion by continuous movements, Proc. London Math. Soc. s**2-20**, 196 (1922).

[22] R. P. Feynman and A. R. Hibbs, *Quantum Mechanics and Path Integrals* (McGraw-Hill, New York, 1965), p. 35.

[23] M. Kac, A stochastic model related to the telegrapher's equation, Rocky Mount. J. Math. **4**, 497 (1974).

[24] J. Masoliver and G. H. Weiss, First passage times for a generalized telegrapher's equation, Physica A **183**, 537 (1992).

[25] G. H. Weiss, Some applications of persistent random walks and the telegrapher's equation, Physica A **311**, 381 (2002).

[26] P. Hänggi and P. Jung, Colored noise in dynamical systems, Adv. Chem. Phys. **89**, 239 (1995).

[27] A. Dhar and D. Chaudhuri, Triple minima in the free energy of semiflexible polymers, Phys. Rev. Lett. **89**, 065502 (2002).

[28] J. Samuel and S. Sinha, Elasticity of semiflexible polymers, Phys. Rev. E **66**, 050801(R) (2002).

[29] J. Tailleur and M. E. Cates, Statistical mechanics of interacting run-and-tumble bacteria, Phys. Rev. Lett. **100**, 218103 (2008).

[30] M. E. Cates and J. Tailleur, Motility-induced phase separation, Annu. Rev. Condens. Matter Phys. **6**, 219 (2015).

[31] L. Angelani, Run-and-tumble particles, telegrapher's equation and absorption problems with partially reflecting boundaries, J. Phys. A: Math. Theor. **48**, 495003 (2015).

[32] C. Bechinger, R. Di Leonardo, H. Löwen, C. Reichhardt, G. Volpe, and G. Volpe, Active particles in complex and crowded environments, Rev. Mod. Phys. **88**, 045006 (2016).

[33] K. Malakar, V. Jemseena, A. Kundu, K. Vijay Kumar, S. Sabhapandit, S. N. Majumdar, S. Redner, and A. Dhar, Steady state, relaxation and first-passage properties of a run-and-tumble particle in one-dimension, J. Stat. Mech. (2018) 043215.

[34] T. Demaerel and C. Maes, Active processes in one dimension, Phys. Rev. E **97**, 032604 (2018).

[35] A. Dhar, A. Kundu, S. N. Majumdar, S. Sabhapandit, and G. Schehr, Run-and-tumble particle in one-dimensional confining potential: Steady state, relaxation and first passage properties, Phys. Rev. E **99**, 032132 (2019).

[36] G. Gradenigo and S. N. Majumdar, A first-order dynamical transition in the displacement distribution of a driven run-and-tumble particle, J. Stat. Mech. (2019) 053206.

[37] F. Mori, P. Le Doussal, S. N. Majumdar, and G. Schehr, Condensation transition in the late-time position of a run-and-tumble particle, Phys. Rev. E **103**, 062134 (2021).

[38] D. S. Dean, S. N. Majumdar, and H. Schawe, Position distribution in a generalized run-and-tumble process, Phys. Rev. E **103**, 012130 (2021).

[39] *Handbook of Mathematical Functions with Formulas, Graphs, and Mathematical Tables*, edited by M. Abramowitz and I. A. Stegun (Dover, New York, 1965).

[40] D. T. Gillespie, A general method for numerically simulating the stochastic time evolution of coupled chemical reactions, J. Comput. Phys. **22**, 403 (1976).

[41] S. N. Majumdar and A. J. Bray, Persistence with partial survival, Phys. Rev. Lett. **81**, 2626 (1998).

[42] A. J. Bray, S. N. Majumdar, and G. Schehr, Persistence and first-passage properties in nonequilibrium systems, Adv. Phys. **62**, 225 (2013).

[43] G. Schehr and S. N. Majumdar, Statistics of the number of zero crossings: From random polynomials to the diffusion equation, Phys. Rev. Lett. **99**, 060603 (2007).

[44] G. Schehr and S. N. Majumdar, Real roots of random polynomials and zero crossing properties of diffusion equation, J. Stat. Phys. **132**, 235 (2008).

[45] M. Poplavskyi and G. Schehr, Exact persistence exponent for the $2D$-diffusion equation and related Kac polynomial, Phys. Rev. Lett. **121**, 150601 (2018).

[46] S. N. Majumdar, P. von Bomhard, and J. Krug, Exactly solvable record model for rainfall, Phys. Rev. Lett. **122**, 158702 (2019).

[47] M. R. Evans, S. N. Majumdar, and G. Schehr, An exactly solvable predator prey model with resetting, J. Phys. A: Math. Theor. **55**, 274005 (2022).

[48] M. Biroli, H. Larralde, S. N. Majumdar, and G. Schehr, Extreme statistics and spacing distribution in a Brownian gas correlated by resetting, Phys. Rev. Lett. **130**, 207101 (2023).

[49] M. Biroli, M. Kulkarni, S. N. Majumdar, and G. Schehr, Dynamically emergent correlations between particles in a switching harmonic trap, Phys. Rev. E **109**, L032106 (2024).